IEEE Access
Multidisciplinary | Rapid Review | Open Access Journal

Received November 7, 2019, accepted November 22, 2019, date of publication November 26, 2019, date of current version December 11, 2019.

Digital Object Identifier 10.1109/ACCESS.2019.2955980

Multi-frequency Vibration Synchronization and Stability of the Nonlinear Screening System

LINGXUAN LI AND XIAOZHE CHEN
School of Control Engineering, Northeastern University at Qinhuangdao, Qinhuangdao 066004, China
Corresponding author: Lingxuan Li (lingxuan_li@163.com)

This work was supported in part by the National Natural Science Foundation of China under Grant 51305070 and Grant 51905081, and in part by the Natural Science Foundation of Hebei Province under Grant E2019501117.

ABSTRACT For vibrating screen machinery, the granular block material can be quickly loosed and fully layered when entering the screening equipment if it is placed an exciting system with low frequency and large amplitude at the feeding end. A high frequency with small amplitude exciter is set near the discharging end. It can make the material appear high-frequency vibration and reduce the phenomenon more effectively that the granular material blocks the screen hole. Because of this, taking the elliptical vibrating screen system as our research object, the concept of compound nonlinear screening trajectories is proposed from the two times frequency vibrating synchronization system driven by three exciters. Firstly, the differential motion equation of the system is obtained by establishing the Laplace equations of the system. Then, by introducing small parameters and dimensionless time parameters, the first-order differential motion equations of the driving motor of the exciters are obtained, the second approximate motion equation of the system is obtained by applying the principle of the average method. Based on this, the criterion for the system to achieve the multi-frequency vibration synchronization state and the phase difference relations among the exciters at steady-state are drawn out by taking the two times frequency vibration synchronization as an example. Meanwhile, the stability criterion of the vibration synchronization state of the system is analyzed. Besides, the functional relation that the location and the rotational direction of the exciters influence on the phase difference of the exciters are given out. Finally, the correctness of the theoretical research is verified by experimental research; the prospect of engineering application of the system is discussed.

INDEX TERMS Synchronization, stability, vibrating screen, multi-frequency, phase difference.

I. INTRODUCTION

Since the 1950s, Blehman has installed two inertial exciters driven by two motors on a single vibration body. He has found that two exciters can rotate in an asynchronous way when some conditions are met. Through theoretical analysis, he has explained the physical mechanism of vibration synchronization of the mechanical system, gradually formed the theory of vibration synchronization and self-synchronization of the mechanical system [1], [2]. The academic definition of synchronization in the sense of kinematics and dynamics is also given by Blekhman [3], [4]. Based on this theory, the synchronization machinery of traditional rigid transmission (e.g., gear transmission) and flexible transmission (e.g., chain or belt transmission) are gradually reduced, replaced by vibration synchronization equipment driven by two or more exciters. They enable the vibrating system to achieve linear motion trajectory, elliptical motion trajectory and other kinds of nonlinear trajectories through vibrating synchronization.

Various motion trajectories of the body of the vibrating system mainly depend on the stable phase differences between the eccentric blocks of the exciters when the system operates at the steady-state. Usually, when the phase differences between the exciters are close to 0 degrees, the system obtains in-phase vibration synchronization. Instead, the system realizes anti-phase vibration synchronization when the phase difference is close to 180 degrees [5]–[12]. For the equipment working in in-phase synchronization, the system can obtain the linear, circle or elliptical motion trajectories; correspondingly, the equipment of linear vibrating screen, circle vibrating screen, the elliptical vibrating screen appear. The elliptical vibrating screen is a new type of screen with

The associate editor coordinating the review of this manuscript and approving it for publication was Yingxiang Liu.

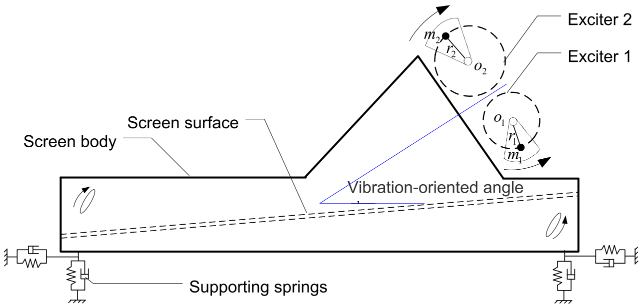

FIGURE 1. **Elliptic vibrating screen with two exciters.**

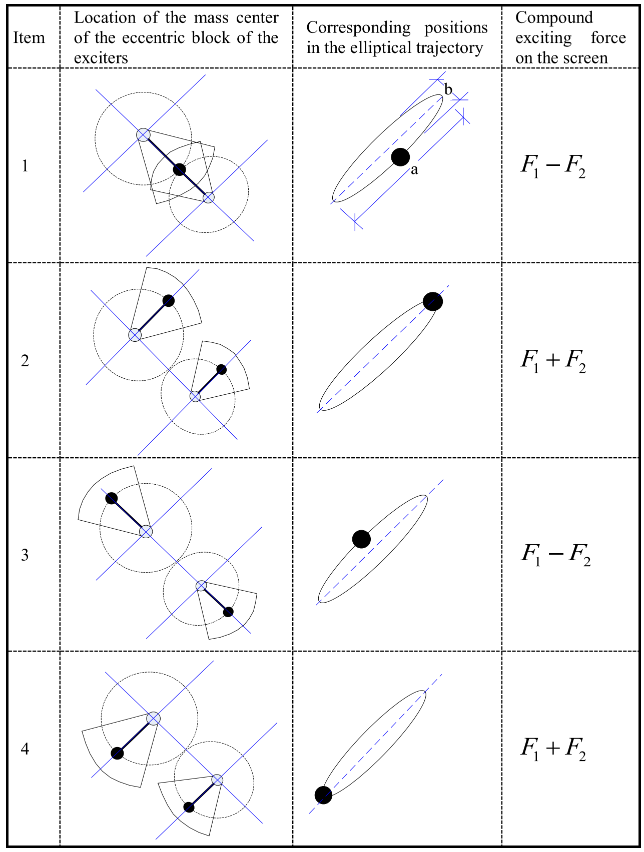

FIGURE 2. **The working principle of the exciters of elliptic vibrating screen driven by two exciters.**

the advantage of both circular and linear trajectory screening system.

On the one hand, the granular material is thrown by the vibrating screen surface, and the rotating acceleration of the material changes continuously in the circumferential direction, which is conducive to the loose stratification of the material and can prevent the material from blocking the screen hole. On the other hand, the material is thrown forward continuously along with the moving screen surface, which makes the equipment have a strong forward conveying capacity. Thus, its screening efficiency and productivity are improved compared with the circular vibrating screen and the linear vibrating screen [13].

The elliptical trajectory of the vibrating screen is usually realized in two different ways. One is that two asymmetric exciters with different exciting mass and rotation radius rotate in reverse rotation direction for achieving an in-phase vibration synchronization state, its typical structure is shown in FIGURE 1; another way is to install three exciters in a vibrating platform system, one of which has different rotating direction from the other two. The latter design is mainly used to solve the problem of insufficient power of the two exciters in some large-scale vibration screening system. Since the latter only increases the exciting force on the long axis of the vibration direction angle, the more representative elliptical vibration screening system driven by two exciters is selected as the research object of this manuscript.

When the two exciters operate synchronously at the rotational velocity of ω rad/s, the long axis (denoted by a) and the short axis (denoted by b) of the trajectory of the mass-center can be calculated by

$$a = \frac{(m_1 r_1 + m_2 r_2)\omega^2}{k_a - M\omega^2}, b = \frac{(m_1 r_1 - m_2 r_2)\omega^2}{k_b - M\omega^2} \tag{1}$$

where, M_i, r_i are the mass and eccentric radius of the eccentric block of the exciter $i(i = 1, 2)$, respectively. m is the mass of the frame, M is the total mass of the system, i. e., $M = m + m_1 + m_2$, k_a and k_b are the stiffness of the system in the vibration-oriented direction and the corresponding vertical direction, respectively. FIGURE 2 plots out the basic working principle of the elliptic vibrating screen driven by two exciters.

As can be seen from (1) and FIGURE 2, the ratio of the long axis to the short axis of the elliptical trajectory of the mass-center of the vibrating system depends mainly on the value of mass m_i and the eccentric radius r_i of the eccentric block of the exciters for the given working speed. For different screening materials, the size of the block granular particle diameter and the degree of viscosity are different, which makes the system need to adjust m_i, $r_i, i\,(i = 1, 2)$. It is disadvantageous for the vibrating system with a fixed ratio $a : b$. Moreover, to make the granular materials quickly loosed and fully layered when they enter the screening equipment, it is necessary to make the exciting force have a low frequency with a large amplitude at the feeding end. Meanwhile, for vibrating screen machinery at the discharging end, a high frequency with small amplitude exciting force is favored to reduce the phenomenon that the granular material blocks the screen hole to improve the screening more efficiently. Besides, Modrzewski and Wodzinski et al. have been engaged in research on the progress of screening of the double-frequency screening system and find that the application of the double-frequency screen can improve the screening process comparing to the single frequency exciting system [14], [15]. Given the above reasons, it is necessary to study the multi-frequency vibration synchronization to design a new type of vibration screening system with compound exciting frequency for obtaining a more complex motion trajectory.

At present, the theory of fundamental frequency vibration synchronization is relatively mature. It mainly includes two types' research methods: the direct motion separation methods represented by Blehman *et al.* [1], [3], [4], [16] and the small parameter average methods represented by Zhang *et al.* [8], [9], [17]–[19]. It is worth noting that the theory of multi-frequency vibration synchronization has seldom been studied in detail by researchers. There are some types of mechanical equipment with multiple exciting frequencies in engineering, such as double-frequency vibrating compactor, multi-frequency vibrating feeder, multi-axis inertial shaker [13]. However, most of them use gears or other transmission mechanisms to achieve the forced multi-frequency synchronization state. The rigid forced synchronization in mechanical structure increases the complexity of the system and reduces the reliability and stability of the vibrating system. Therefore, the development of multi-frequency vibration synchronization theory is particularly important. As early as the 1980s, Japanese researchers Inoue and Araki arranged four exciting motors symmetrically on a vibrating system, observed the phenomenon of two times frequency synchronization and three times frequency synchronization, and deduced the related theory [20]. Unfortunately, this theoretical research has not been paid much attention to the asymmetrically vibrating system. Subsequently, Wen had pointed out that some nonlinear systems could achieve the multi-frequency synchronization state in the 1980s. The system designed by Wen has a double vibration mass; each one has two degrees of freedom, supported by piecewise nonlinear springs [13]. On the one hand, this system has a relatively complex mechanical structure; on the other hand, it rests in the conceptual phases of product design and hasn't proved the reliability by experiments.

The difficulty in the design of the multi-frequency vibration synchronization system is just as Wen pointing out. It is more difficult to implement the entrainment of high order harmonic frequency and the subharmonic frequency capture than fundamental frequency capture because of the smaller frequency capture interval [13]. Therefore, Jia et al. has been investigated the control synchronization of the vibrating system in the view of controlling the rotational speed and phase of the driving motor of the exciter and achieved a stable state of synchronization [21]–[23]. Compared to realizing the synchronization of the vibration system by control synchronization theory, the vibration synchronization have obvious advantages in assuring stability and reliability of the system and cost savings. The theory of control synchronization is still not mature. We only find that the vibrating cone crusher of FCB Rhodax®4D has controlled the grinding force; it may use the theory of control synchronization [24]. If the system can be controlled based on optimum structural parameters, the stability and robustness of the system can be greatly improved, the energy loss caused by forced control can be reduced. Therefore, it is urgent to study the theory of multi-frequency vibration synchronization and give out the critical structural parameters. Recently, Zou has studied the self-synchronous vibration system with dual-frequency and dual-motor excitation [25].

In our previous research, a vibrating system with two exciters rotating in opposite directions was investigated. The condition of multi-frequency vibration synchronization and its stability criterion were obtained; the feasibility was also proved by experiment studies [26]. Besides, a multi-frequency vibrating system with two homodromy exciters was also studied. We find that the system exists bistable phase difference intervals and give out the critical structural parameters and corresponding criterions. Furthermore, the possible engineering application direction was also explored by adding a feeding material chamber to observe the motion trajectories of particle materials.

To further explore the application of multi-frequency vibration synchronization theory, this paper studies on the basis of nonlinear vibrating screen to improve the effect of material rapid loosening and stratification at the feeding end and block granular material rapid separation at the discharging end. The full text is divided into four parts. The first section mainly introduces the relevant engineering background and research status of multi-frequency vibration synchronization. The second section carries out the dynamic modeling of the vibration synchronization system. After taking two times-frequency vibration synchronization as an example, the conditions of realizing vibration synchronization are deduced, the stability of the synchronization state is also carried out. In the third section, the feasibility of theoretical analysis is verified by an experimental study; the issue of engineering application is discussed. Finally, in the fourth section, the main conclusions of this study are summarized.

II. THEORETICAL RESEARCH

A. WORKING PRINCIPLE OF MULTI-FREQUENCY NONLINEAR VIBRATING SCREEN

Based on the conception mentioned above, a multi-frequency nonlinear screening system is proposed according to the elliptic vibrating screen. Its mechanical model is shown in FIGURE 3.

where, oxy is the fixed coordinate system, m is the mass of the frame, o is the mass center of the whole vibrating

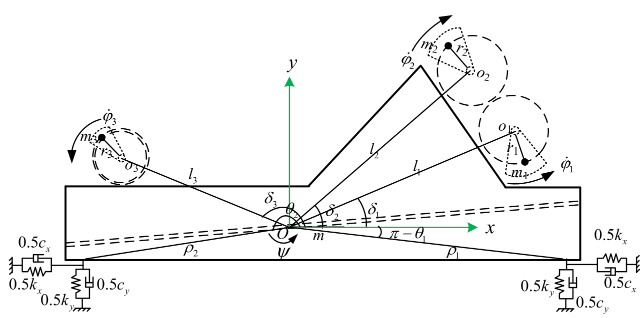

FIGURE 3. Dynamic model of the vibrating system driven three exciters powered by multi-frequency.

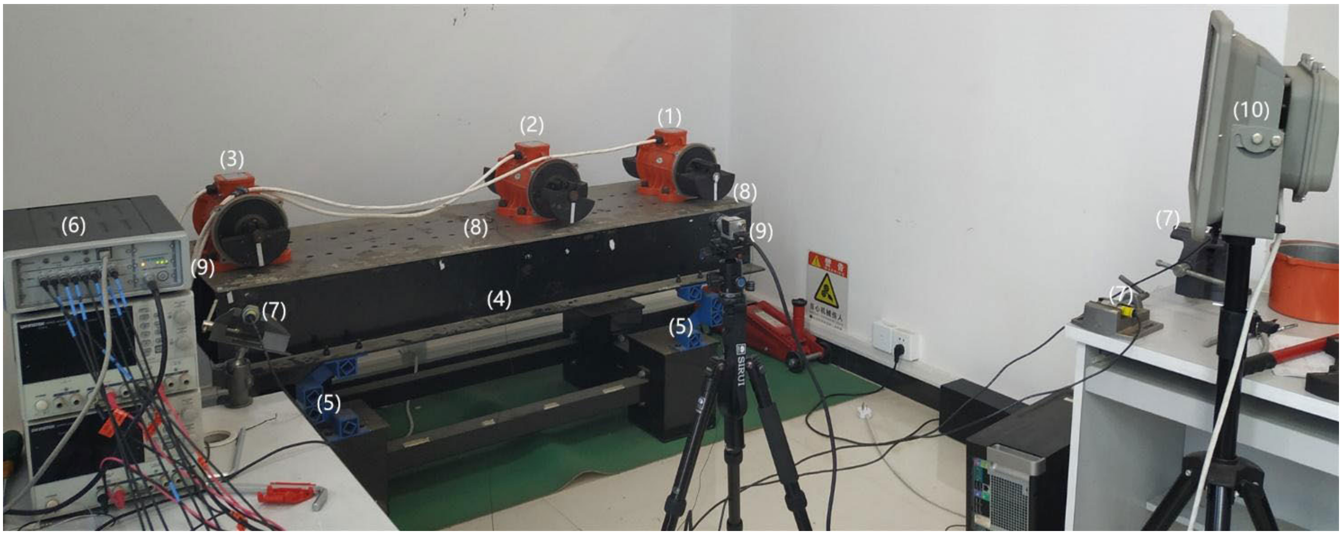

FIGURE 4. **Multi-frequency vibration synchronization experimental system. (1). Exciter 1, (2). Exciter 2, (3). Exciter 3, (4). Rigid frame of the system, (5). Four springs with the type of ROSTA AB27, (6). Signal acquisition system, (7). Three ROLS remote optical laser sensors, (8). Three triaxial accelerometers, (9). Basler acA1440-220uc camera, (10). Supplement light system for the camera.**

system, k_x, k_y and c_x, c_y are the stiffness and damping of the system in x, y direction, respectively. $\rho_i, \theta_i\,(i=1,2)$ are the distance from connecting point between spring and frame to point o and the angle between its connection and the horizontal direction. $\dot{\varphi}_i$ and φ_i are the instantaneous angular velocity and the rotational angle relative to the starting point of the exciter $i\,(i=1,2,3)$, respectively. l_i and δ_i are the distance from the axis of the exciter $i\,(i=1,2,3)$ to the mass center o of the system and the angle between its connection and the horizontal direction. When the high-frequency Exciter 3 is directly located above the mass center of the system, that is $\delta_3 = {}^{\pi}\!/_{2}$, the exciter mainly affects the trajectory of the mass center. The Exciter 3 will affect the trajectory of the discharge end of the vibrating system when $\delta_3 > {}^{\pi}\!/_{2}$.

For the elliptic vibrating screen, there must have the relations of $m_2r_2 > m_1r_1$ or $m_2r_2 < m_1r_1$ between the Exciter 1 and the Exciter 2. Exciter 3 has a higher exciting frequency and lower exciting force. Most of the driving motor of the exciter in the vibrating system is three-phase induction motor, and its maximum synchronous speed is 3000r/min, the multi-frequency relations is usually limited to two or three times. In the following section, only a two times-frequency example is mainly used to analyze the dynamic characteristics, synchronization state and its stability.

B. DIFFERENTIAL MOTION EQUATIONS

Based on FIGURE 3, the equation of kinetic, potential energy and energy dissipate function of the system are given as follows.

$$
\begin{aligned}
T &= \frac{1}{2}m\left(\dot{x}^2+\dot{y}^2\right)+\frac{1}{2}J_m\dot{\psi}^2+\frac{1}{2}\sum_{i=1}^{3}J_i\dot{\varphi}_i^2\\
&\quad+\frac{1}{2}\sum_{i=1}^{3}m_i\begin{Bmatrix}\left[\dot{x}-l_i\dot{\psi}\sin\left(\beta_i+\psi\right)-r_i\dot{\varphi}_i\sin\varphi_i\right]^2\\+\left[\dot{y}+l_i\dot{\psi}\cos\left(\beta_i+\psi\right)+r_i\dot{\varphi}_i\cos\varphi_i\right]^2\end{Bmatrix}\\
V &= \frac{1}{2}\sum_{i=1}^{2}\begin{Bmatrix}k_{xi}\left[x-\rho_i\psi\sin\left(\theta_i+\psi\right)\right]^2\\+k_{yi}\left[-y-\rho_i\psi\cos\left(\theta_i+\psi\right)\right]^2\end{Bmatrix}\\
&\quad+\frac{1}{2}\sum_{i=1}^{3}m_igr_i\cos\varphi_i\\
D_0 &= \frac{1}{2}\sum_{i=1}^{2}\begin{Bmatrix}c_{xi}\left[\dot{x}-\rho_i\dot{\psi}\sin\left(\theta_i+\psi\right)\right]^2\\+c_{yi}\left[-\dot{y}-\rho_i\dot{\psi}\cos\left(\theta_i+\psi\right)\right]^2\end{Bmatrix}\\
&\quad+\frac{1}{2}\sum_{i=1}^{3}c_{di}\dot{\varphi}_i^2
\end{aligned}
\tag{2}
$$

where, J_m is the moment of inertia of the rigid frame of the system, J_i is the moment of inertia of the Exciter i, c_{di} is the damping coefficient of the exciter $i(i=1,2,3)$. β_i is the coefficient related to δ_i and the rotational direction of Exciter i, that is, $\beta_i = \delta_i$ when the Exciter i rotates in counter-clockwise direction towards the origin of its axis; otherwise, $\beta_i = \pi - \delta_i$. The symbol ($\bullet$) above the parameter denotes taking its derivatization with respect to time t.

For the vibrating system (such as the experiment platform in FIGURE 4), the length of the body is 1600mm, the maximum amplitude is about 6mm. The angular displacement ψ is 0.01rad; the minimum value of β_i and $\theta_i\,(i=1,2)$ is β_1(about 0.18rad°). Thus, the angular displacement ψ can be ignored. In addition, the theory of vibration synchrozation are mainly used to design the screening system. Usually, the amplitude of the screening system is less than 10mm. Meanwhile, the length of the vibrating screens is too long (For example, length of Schenck Process linear vibrating screens: 4,800-11,500 mm). To sum up, the angular displacement ψ is to small compared toβ_i and $\theta_i\,(i=1,2)$.

Considering that the angular displacement ψ of the system is too small comparing with β_i and $\theta_i\,(i=1,2)$, it can be left out when calculating the kinetic energy of the system and the potential of the springs. Choose $x, y, \psi, \varphi_i, (i = 1, 2, 3)$ as generalized coordinate, and substitute (2) to Lagrange equation, as shown in (3).

$$\frac{\mathrm{d}}{\mathrm{d}t}\frac{\partial(T-V)}{\partial \dot{q}_{\mathrm{i}}} - \frac{\partial(T-V)}{\partial q_{\mathrm{i}}} + \frac{\partial D_0}{\partial \dot{q}_{\mathrm{i}}} = Q_{\mathrm{i}} \tag{3}$$

Then, the differential equation of motion of the system is obtained.

$$\begin{aligned}
&M\ddot{x} + c_x\dot{x} + k_x x - c_{x\psi}\dot{\psi} - k_{x\psi}\psi \\
&\quad = \sum_{i=1}^{3}\sigma_i m_i r_i\left(\dot{\varphi}^2\cos\varphi_i + \ddot{\varphi}\sin\varphi_i\right) \\
&\qquad + \sum_{i=1}^{3} m_i l_i\left(\dot{\psi}^2\cos\beta_i + \ddot{\psi}\sin\beta_i\right) \\
&M\ddot{y} + c_y\dot{y} + k_y y + c_{y\psi}\dot{\psi} + k_{y\psi}\psi \\
&\quad = \sum_{i=1}^{3} m_i r_i\left(\dot{\varphi}^2\sin\varphi_i - \ddot{\varphi}\cos\varphi_i\right) \\
&\qquad + \sum_{i=1}^{3} m_i l_i\left(\dot{\psi}^2\sin\beta_i - \ddot{\psi}\cos\beta_i\right) \\
&J_\psi\ddot{\psi} + c_\psi\dot{\psi} + k_\psi\psi - c_{x\psi}\dot{x} + c_{y\psi}\dot{y} - k_{x\psi}x + k_{y\psi}y \\
&\quad = \sum_{i=1}^{3} m_i l_i\left\{\begin{array}{l} r_i\left[\dot{\varphi}^2\sin(\varphi_i-\beta_i) - \ddot{\varphi}\cos(\varphi_i-\beta_i)\right] \\ + (\ddot{x}\sin\beta_i - \ddot{y}\cos\beta_i)\end{array}\right\} \\
&J_{di}\ddot{\varphi}_i + c_{di}\dot{\varphi}_i \\
&\quad = m_i r_i\left[\begin{array}{l}\left(\ddot{x} - l_i\ddot{\psi}\sin\beta_i - l_i\dot{\psi}^2\cos\beta_i - \frac{g}{2}\right)\sin\varphi_i \\ + \left(-\ddot{y} - l_i\ddot{\psi}\cos\beta_i + l_i\dot{\psi}^2\sin\beta_i\right)\cos\varphi_i\end{array}\right] \\
&\qquad + L_i,\ i = 1, 2, 3
\end{aligned} \tag{4}$$

where, L_i is the output torque of the motor of the exciter $i\,(i = 1, 2, 3)$. $M = m + \sum_{i=1}^{3} m_i$,

$$\begin{aligned}
J_\psi &= J_m + \sum_{i=1}^{3} m_i l_i^2,\ J_{di} = J_i + m_i r_i^2,\ (\ i = 1, 2, 3\ ), \\
k_x &= k_{x1} + k_{x2},\ k_y = k_{y1} + k_{y2}, \\
c_x &= c_{x1} + c_{x2},\ c_y = c_{y1} + c_{y2}, \\
k_{x\psi} &= k_{x1}\rho_1\sin\theta_1 + k_{x2}\rho_2\sin\theta_2, \\
k_{y\psi} &= k_{y1}\rho_1\cos\theta_1 + k_{y2}\rho_2\cos\theta_2, \\
k_\psi &= k_{x1}\rho_1^2\sin^2\theta_1 + k_{x2}\rho_2^2\sin^2\theta_2 + k_{y1}\rho_1^2\cos^2\theta_1 \\
&\quad + k_{y2}\rho_2^2\cos^2\theta_2, \\
c_{x\psi} &= c_{x1}\rho_1\sin\theta_1 + c_{x2}\rho_2\sin\theta_2, \\
c_{y\psi} &= c_{y1}\rho_1\cos\theta_1 + c_{y2}\rho_2\cos\theta_2, \\
c_\psi &= c_{x1}\rho_1^2\sin^2\theta_1 + c_{x2}\rho_2^2\sin^2\theta_2 + c_{y1}\rho_1^2\cos^2\theta_1 \\
&\quad + c_{y2}\rho_2^2\cos^2\theta_2.
\end{aligned}$$

C. PARAMETERIZATION OF THE DIFFERENTIAL EQUATIONS

Considering that the working speed of the driving motor of the exciter is much higher than the natural frequency of the vibrating system and the symmetrical arrangement of the elastic spring support system. According to the previous research references [13], [17], it is desirable to adopt $k_{x\psi} = k_{y\psi} = 0$, $c_{x\psi} = c_{y\psi} = 0$, which can ensure the required accuracy of engineering calculation. At the same time, due to the vibration synchronization system belongs to a typical weak damping system, the small damping terms of the first three equations in (4) can be neglected. Then, take the derivatives of the first three equations respect to time t and substitute them into the motor equation of the latter two equations of (4) [20] and take small parameters as

$$\varepsilon = r_m r^2\frac{m_1}{J_1} \tag{5}$$

we have

$$\ddot{\varphi}_j = \varepsilon\left\{\begin{array}{l}
\omega^2\sigma_i T_i - 2\omega\alpha_i\dot{\varphi}_i - \omega^2 k_i\sin\varphi_i \\
+\sum_{j=1}^{3} a_{ij}\left[\dot{\varphi}_j^2\sin(\varphi_i-\varphi_j) + \ddot{\varphi}_j\cos(\varphi_i-\varphi_j)\right] \\
-\sum_{j=1}^{3} a_{ij}b_{ij}\dot{\varphi}_j^2\left\{\begin{array}{l}\left[\begin{array}{l}\sin(\varphi_i+\varphi_j-\beta_i-\beta_j) \\ +\sin(\varphi_i-\varphi_j-\beta_i+\beta_j)\end{array}\right] \\ +\ddot{\varphi}_j\left[\begin{array}{l}\cos(\varphi_i+\varphi_j-\beta_i-\beta_j) \\ +\cos(\varphi_i-\varphi_j-\beta_i+\beta_j)\end{array}\right]\end{array}\right\} \\
-\sum_{j=1}^{3} a_{ij}c_{ij}\dot{\varphi}_j^2\left[\begin{array}{l}\sin(\varphi_i+2\varphi_j-\beta_i-2\beta_j) \\ +\sin(\varphi_i-2\varphi_j-\beta_i+2\beta_j) \\ -2\sin(\varphi_i-\beta_i)\end{array}\right]
\end{array}\right\} \tag{6}$$

where,

$$\begin{aligned}
a_{ij} &= \frac{J_1 m_i m_j r_i r_j}{J_i m_1^2 r_1^2},\ b_{ij} = \frac{M l_i l_j}{2J_\psi},\ c_{ij} = \frac{m_j r_j l_i l_j^2 M}{4J_\psi^2}, \\
k_i &= \frac{m_i r_i g J_1 M}{2J_i\omega^2 m_1^2 r_1^2},\ \alpha_i = \frac{J_1 M f_{di}}{2J_i\omega m_1^2 r_1^2},\ T_i = \frac{J_1 M L_i}{J_i\omega^2 m_1^2 r_1^2}.
\end{aligned}$$

Set the basic angular velocity of the three exciters is ω when the motors of the exciters of the vibrating system achieve a steady operating point. Its small phase fluctuation can be regarded as a slowly varying parameter of time, which is $\vartheta_i\ (i = 1, 2, 3)$ respectively, then the phase of the exciter φ_i should be

$$\varphi_i(t) = \sigma_i n_i\omega t + \sigma_i\vartheta_i(t),\ i = 1, 2, 3 \tag{7}$$

Now dimensionless time τ is introduced to replace the time t measured in seconds. Its unit is the ratio of the vibration period of the vibration item to 2π, that is $1/\omega$. Thus,

$$\tau = \omega t,\quad \frac{d}{d\tau} = \frac{1}{\omega}\frac{d}{dt},\quad \frac{d^2}{d\tau^2} = \frac{1}{\omega^2}\frac{d^2}{dt^2} \tag{8}$$

To apply the principle of the averaging method, (6) can be transformed into the standard form advocated by Bogolubov by letting [27]

$$\begin{aligned}
\vartheta_i &= \vartheta_i \\
\frac{d\vartheta_i}{d\tau} &= \sqrt{\varepsilon}\,\nu_i
\end{aligned} \tag{9}$$

When the higher-order minor terms such as $\varepsilon\dot{\vartheta}_j$ are ignored, the second-order differential equation of (6) can be transformed into the first-order differential equation as

$$
\begin{aligned}
&\frac{d\vartheta_i}{d\tau} = \sqrt{\varepsilon}\,\nu_i \\
&\sigma_i\frac{d\nu_i}{d\tau} = \sqrt{\varepsilon}\left[\sigma_i\left(T_i - 2n_i\alpha_i\right) - k_i\sin\left(\sigma_i n_i\tau + \sigma_i\vartheta_i\right)\right] \\
&+\sqrt{\varepsilon}\sum_{i=1}^{3} a_{ij}n_j^2\left\{\begin{array}{l}\sin\left(\theta_{1ij} + \beta_i - \beta_j\right) \\ \quad + b_{ij}\left(\sin\theta_{1ij} - \sin\theta_{2ij}\right) \\ -c_{ij}\left[\begin{array}{l}\sin\theta_{3ij} + \sin\theta_{4ij} \\ +2\sin\left(\sigma_i n_i\tau + \sigma_i\vartheta_i - \beta_i\right)\end{array}\right]\end{array}\right\} \\
&-2\varepsilon\alpha_i\nu_i\sigma_i + 2\varepsilon a_{ij}n_j\nu_j\left\{\begin{array}{l}2\sin\left(\theta_{1ij} + \beta_i - \beta_j\right) \\ \quad + b_{ij}\left(\sin\theta_{1ij} - \sin\theta_{2ij}\right) \\ -2c_{ij}\left[\begin{array}{l}\sin\theta_{3ij} + \sin\theta_{4ij} \\ +2\sin \\ \quad\left(\sigma_i n_i\tau + \sigma_i\vartheta_i - \beta_i\right)\end{array}\right]\end{array}\right\} \\
&+\sqrt{\varepsilon^3}a_{ij}\nu_j^2\left\{\begin{array}{l}\sin\left(\theta_{1ij} + \beta_i - \beta_j\right) \\ \quad + b_{ij}\left(\sin\theta_{1ij} - \sin\theta_{2ij}\right) \\ -c_{ij}\left[\begin{array}{l}\sin\theta_{3ij} + \sin\theta_{4ij} \\ +2\sin\left(\sigma_i n_i\tau + \sigma_i\vartheta_i - \beta_i\right)\end{array}\right]\end{array}\right\}
\end{aligned} \tag{10}
$$

where,

$$
\begin{aligned}
\theta_{1ij} &= \tau n_i\sigma_i - \tau n_j\sigma_j + \sigma_i\vartheta_i - \sigma_j\vartheta_j - \beta_i + \beta_j, \\
\theta_{2ij} &= \tau n_i\sigma_i + \tau n_j\sigma_j + \sigma_i\vartheta_i + \sigma_j\vartheta_j - \beta_i - \beta_j, \\
\theta_{3ij} &= \tau n_i\sigma_i - 2\tau n_j\sigma_j + \sigma_i\vartheta_i - 2\sigma_j\vartheta_j - \beta_i + 2\beta_j, \\
\theta_{4ij} &= \tau n_i\sigma_i + 2\tau n_j\sigma_j + \sigma_i\vartheta_i + 2\sigma_j\vartheta_j - \beta_i - 2\beta_j.
\end{aligned}
$$

The term $\frac{d\nu_i}{d\tau}$ in (10) can be regarded as the slow variable functions proportional to $\sqrt{\varepsilon}$, i.e., ν_i is the sum of the stationary term and the high-order minor vibration term. Since the latter terms are very small, we have its first approximation

$$
\begin{aligned}
&\vartheta_i = \vartheta_i \\
&\sigma_i\nu_i = \sigma_i\Omega_i + \sqrt{\varepsilon}\frac{k_i\cos\left(\sigma_i n_i\tau + \sigma_i\vartheta_i\right)}{\sigma_i n_i} \\
&\quad -\sqrt{\varepsilon}\sum_{j=1}^{3} a_{ij}n_j^2\left\{\begin{array}{l}p_{1ij}\cos\left(\theta_{1ij} + \beta_i - \beta_j\right) \\ \quad - b_{ij}\left(p_{1ij}\cos\theta_{1ij} - p_{2ij}\cos\theta_{2ij}\right) \\ -c_{ij}\left[\begin{array}{l}p_{3ij}\cos\theta_{3ij} + p_{4ij}\cos\theta_{4ij} \\ +\dfrac{2\cos\left(\tau n_i\sigma_i + \sigma_i\vartheta_i - \beta_i\right)}{\sigma_i n_i}\end{array}\right]\end{array}\right\}
\end{aligned} \tag{11}
$$

where, Ω_i is a time related function introduced according to the asymptotic methods in nonlinear vibration theory [20], [27]. In (11),

when $n_i\sigma_i - n_j\sigma_j \neq 0$, $p_{1ij} = \left(n_i\sigma_i - n_j\sigma_j\right)^{-1}$, otherwise $p_{1ij} = 0$;

when $n_i\sigma_i + n_j\sigma_j \neq 0$, $p_{2ij} = \left(n_i\sigma_i + n_j\sigma_j\right)^{-1}$, otherwise $p_{2ij} = 0$;

when $n_i\sigma_i - 2n_j\sigma_j \neq 0$, $p_{3ij} = \left(n_i\sigma_i - 2n_j\sigma_j\right)^{-1}$, otherwise $p_{3ij} = 0$;

when $n_i\sigma_i - 2n_j\sigma_j \neq 0$, $p_{2ij} = \left(n_i\sigma_i + n_j\sigma_j\right)^{-1}$, otherwise $p_{4ij} = 0$.

Similarly, the improved second approximation can be obtained as

$$
\begin{aligned}
&\vartheta_i = \vartheta_i \\
&\sigma_i\nu_i = \sigma_i\Omega_i + \sqrt{\varepsilon}\frac{k_i\cos\left(\sigma_i n_i\tau + \sigma_i\vartheta_i\right)}{\sigma_i n_i} \\
&\quad -\sqrt{\varepsilon}\sum_{j=1}^{3} a_{ij}n_j^2\left\{\begin{array}{l}p_{1ij}\cos\left(\theta_{1ij} + \beta_i - \beta_j\right) \\ \quad - b_{ij}\left(p_{1ij}\cos\theta_{1ij} - p_{2ij}\cos\theta_{2ij}\right) \\ -c_{ij}\left[\begin{array}{l}p_{3ij}\cos\theta_{3ij} + p_{4ij}\cos\theta_{4ij} \\ +\dfrac{2\cos\left(\tau n_i\sigma_i + \sigma_i\vartheta_i - \beta_i\right)}{\sigma_i n_i}\end{array}\right]\end{array}\right\} \\
&\quad -2\varepsilon\sum_{j=1}^{3} a_{ij}n_j\Omega_j\left\{\begin{array}{l}p_{1ij}\cos\left(\theta_{1ij} + \beta_i - \beta_j\right) \\ \quad + b_{ij}\left(p_{1ij}\cos\theta_{1ij} - p_{2ij}\cos\theta_{2ij}\right) \\ -c_{ij}\left[\begin{array}{l}p_{3ij}\cos\theta_{3ij} + p_{4ij}\cos\theta_{4ij} \\ +\dfrac{\cos\left(\sigma_i n_i\tau + \sigma_i\vartheta_i - \beta_i\right)}{\sigma_i n_i}\end{array}\right]\end{array}\right\}
\end{aligned} \tag{12}
$$

Substitute (12) into (10) and take an average of time τ, consider that the driving motors of the two low-frequency exciters rotate in opposite directions, we obtain the second approximate equation of the system in (10), i.e.,

$$
\begin{aligned}
\frac{d\vartheta_i}{d\tau} &= \sqrt{\varepsilon}\,\Omega_i \\
\sigma_i\frac{d\Omega_i}{d\tau} &= \sqrt{\varepsilon}\left[\sigma_i\left(T_i - 2n_i\alpha_i\right) - \sum_{j=1}^{3} n_j^2 a_{ij}\Delta_{ij}\right] \\
&\quad -2\varepsilon\left[\alpha_i\Omega_i\sigma_i + \sum_{j=1}^{3}\Omega_j a_{ij}n_j\sigma_j\Delta_{ij}\right] \\
&\quad -\sqrt{\varepsilon^3}\sum_{j=1}^{3} k_j\sigma_j a_{ij}\Lambda_{ij} - \sqrt{\varepsilon^3}\cdots
\end{aligned} \tag{13}
$$

where,

$$
\begin{aligned}
\Delta_{ij} &= -u_1 b_{ij}\sin\delta_{1ij} - u_1\sin\left(\delta_{1ij} + \beta_i - \beta_j\right), \\
&\quad +u_2 c_{ij}\sin\delta_{2ij} + u_3 c_{ij}\sin\delta_{3ij} \\
\Lambda_{ij} &= c_{ij}u_1\left[2\sin\left(\delta_{1ij} + \beta_j\right) + \sin\left(\delta_{1ij} - \beta_j\right)\right] \\
&\quad +u_2 b_{ij}\sin\left(\delta_{2ij} + \beta_j\right) \\
&\quad -u_3\left[b_{ij}\sin\left(\delta_{3ij} - \beta_j\right) + \sin\left(\sigma_i\vartheta_i - 2\sigma_j\vartheta_j\right)\right] \\
&\quad +u_4 c_{ij}\sin\delta_{4ij} + u_5 c_{ij}\sin\delta_{5ij}
\end{aligned}
$$

When $n_i\sigma_i + n_j\sigma_j = 0$, $u_1 = 1$, $\delta_{1ij} = \sigma_i\vartheta_i + \sigma_j\vartheta_j - \beta_i - \beta_j$, otherwise, $u_1 = 0$;

When $n_i\sigma_i + 2n_j\sigma_j = 0$, $u_2 = 1$, $\delta_{2ij} = \sigma_i\vartheta_i + 2\sigma_j\vartheta_j - \beta_i - 2\beta_j$, otherwise, $u_2 = 0$;

When $n_i\sigma_i - 2n_j\sigma_j = 0$, $u_3 = 1$, $\delta_{3ij} = \sigma_i\vartheta_i - 2\sigma_j\vartheta_j - \beta_i + 2\beta_j$, otherwise, $u_3 = 0$;

When $n_i\sigma_i + 3n_j\sigma_j = 0$, $u_4 = 1$, $\delta_{4ij} = \sigma_i\vartheta_i + 3\sigma_j\vartheta_j - \beta_i - 2\beta_j$, otherwise, $u_4 = 0$;

When $n_i\sigma_i - 3n_j\sigma_j = 0$, $u_5 = 1$, $\delta_{5ij} = \sigma_i\vartheta_i - 3\sigma_j\vartheta_j - \beta_i + 2\beta_j$, otherwise, $u_5 = 0$.

The coefficients of $\sqrt{\varepsilon}$ and ε in (13) give out the phase relations of the eccentric block of the exciters when the system operates at the steady-state. Then, the phase relations among the exciters at the steady-state can be obtained by letting the related coefficients in (13) equal to 0. Due to the steady-state phase relations and the criterion of stability of same-frequency synchronization has been proved by many references, the following sections mainly focus on the issue of the two times frequency vibration synchronization.

D. PHASE RELATIONS AND STABILITY ANALYSIS OF TWO TIMES FREQUENCY VIBRATION SYNCHRONIZATION

According to FIGURE 3, the Exciter 1 and Exciter 2 are the low-frequency exciters; the Exciter 3 is the high-frequency exciter. For two times frequency vibrating system, assume $n_1 = n_2 = n$, $n_3 = 2n$. Similarly, the rotational direction of the three exciters is $\sigma_1 = 1$, $\sigma_2 = -1$ and $\sigma_3 = 1$, respectively. The $\sqrt{\varepsilon}$ and ε terms of (13) are processed similarly by the methods mentioned above, then, we have

$$\begin{aligned}
\frac{d\vartheta_i}{d\tau} &= \sqrt{\varepsilon}\,\Omega_i \ \ (i=1,2,3)\\
\frac{d\Omega_1}{d\tau} &= (T_1 - 2n\alpha_1)\sqrt{\varepsilon} - 2\alpha_1\Omega_1\varepsilon\\
&\quad + a_{12}b_{12}n\left(n\sqrt{\varepsilon} - 2\Omega_2\varepsilon\right)\sin(-\vartheta_1+\vartheta_2+\beta_1+\beta_2)\\
\frac{d\Omega_2}{d\tau} &= (T_2 - 2n\alpha_2)\sqrt{\varepsilon} - 2\alpha_2\Omega_2\varepsilon\\
&\quad - a_{21}b_{21}n\left(n\sqrt{\varepsilon} + 2\Omega_1\varepsilon\right)\sin(-\vartheta_1+\vartheta_2+\beta_1+\beta_2)\\
\frac{d\Omega_3}{d\tau} &= (T_3 - 2n\alpha_3)\sqrt{\varepsilon} - 2\alpha_3\Omega_3\varepsilon\\
&\quad + a_{32}b_{32}n\left(n\sqrt{\varepsilon} - 2\Omega_2\varepsilon\right)\sin(2\vartheta_2-\vartheta_3+2\beta_2+\beta_3)
\end{aligned} \tag{14}$$

If the system enters the steady working state and assumes the basic angular velocity of three exciters is ω_0, the difference of $T_i - 2n\alpha_i$ between the output torque of driving motor of the exciter and its shaft resistance should approach 0. The slowly varying attenuation term $\vartheta_i (i = 1, 2, 3)$ in the system will approach a constant value $\vartheta_{i0} (i = 1, 2, 3)$, that is, $\frac{d\vartheta_i}{d\tau}$ and $\frac{d\Omega_i}{d\tau}$ are equal to 0. Further, the criterion for the steady motion of the system under two times frequency vibration synchronization is obtained as follows.

$$\begin{aligned}
&\sin(-\vartheta_{10} + \vartheta_{20} + \beta_1 + \beta_2) \approx 0\\
&\sin(2\vartheta_{20} - \vartheta_{30} + 2\beta_2 + \beta_3) \approx 0
\end{aligned} \tag{15}$$

To obtain the relations between the phase coefficient ϑ_{i0} of the exciter i $(i = 1, 2, 3)$ and the phase difference among the exciters at the synchronization state, the perturbation analysis is introduced. The corresponding small perturbation terms are set as μ_i and η_i for ϑ_i and Ω_i, respectively. i.e.,

$$\vartheta_i = \vartheta_{i0} + \mu_i,\ \ \Omega_i = \Omega_{i0} + \eta_i,\ \ (i = 1, 2, 3) \tag{16}$$

Equation (16) substitutes into (10). Then, the nonlinear system is linearized by Taylor expansion; the equivalent perturbation equation is obtained.

TABLE 1. Main parameters of the exciters.

Parameter	*Exciter 1*	*Exciter 2*	*Exciter 3*	*Unit*
Poles	6	6	4	pole
Maximum exciting force	7	5.95	3.5	kN
Eccentric mass of the block of the exciter	14.8	12.6	4.6	kg
Eccentric radius of the eccentric block of the exciter	52.0	52.0	34.5	mm
Rated power	0.37	0.37	0.37	kW
Rated voltage	380	380	380	V
Rated current	1.32	1.32	1.22	A
Rated speed	910	910	1420	r/min
Stator resistance	16.88	16.88	16.94	Ω
Rotor resistance	12.63	12.60	12.63	Ω
Stator inductance	41.77	41.77	41.77	mH
Rotor inductance	40.10	40.10	44.09	mH

$$\begin{aligned}
&\mu_i' = \eta_i\sqrt{\varepsilon} \quad (i = 1, 2, 3)\\
&\eta_1' + 2\varepsilon\alpha_1\eta_1\\
&\quad + a_{12}b_{12}n(\mu_1 - \mu_2)\left(n\sqrt{\varepsilon} - 2\Omega_{20}\varepsilon\right)\\
&\quad \times \cos(\beta_1 + \beta_2 - \vartheta_{10} + \vartheta_{20}) = 0\\
&\eta_2' + 2\varepsilon\alpha_2\eta_2\\
&\quad - a_{21}b_{21}n(\mu_1 - \mu_2)\left(n\sqrt{\varepsilon} + 2\Omega_{10}\varepsilon\right)\\
&\quad \times \cos(\beta_1 + \beta_2 - \vartheta_{10} + \vartheta_{20}) = 0\\
&\eta_3' + 2\varepsilon\alpha_3\eta_3\\
&\quad - a_{32}c_{32}n(2\mu_2 - \mu_3)\left(n\sqrt{\varepsilon} - 2\Omega_{20}\varepsilon\right)\\
&\quad \times \cos(2\beta_2 + \beta_3 + 2\vartheta_{20} - \vartheta_{30}) = 0
\end{aligned} \tag{17}$$

where, μ_i' and η_i' denote the derivation of dimensionless time τ by μ_i and η_i, respectively. According to the theory of linear system [28], the characteristic equation of (17) is established with the variable λ as the characteristic index, then obtain that

$$\lambda\begin{bmatrix}\lambda^2 + 2\alpha_3\varepsilon\lambda\\ +a_{32}c_{32}n^2\varepsilon\cos(2\beta_2 + \beta_3 + 2\vartheta_{20} - \vartheta_{30})\end{bmatrix}
\begin{Bmatrix}\lambda^3 + 2(\alpha_1 + \alpha_2)\varepsilon\lambda^2 + 4\alpha_1\alpha_2\varepsilon^2\lambda\\ + \begin{bmatrix}(2\varepsilon\alpha_2 + \lambda)a_{12}b_{12}\\ +(2\varepsilon\alpha_1 + \lambda)a_{21}b_{21}\end{bmatrix}\\ n^2\varepsilon\cos(\beta_1 + \beta_2 - \vartheta_{10} + \vartheta_{20})\end{Bmatrix} = 0 \tag{18}$$

According to the requirement that all the eigenvalues corresponding to the characteristic (18) of the nonlinear system should satisfy $\mathrm{Re}(\lambda_i) \leq 0$ [20], [29], the stability criterion for the system to achieve the two times frequency vibration synchronization can be listed as follows

$$\begin{aligned}
&\cos(\beta_1 + \beta_2 - \vartheta_{10} + \vartheta_{20}) > 0\\
&\cos(2\beta_2 + \beta_3 + 2\vartheta_{20} - \vartheta_{30}) > 0
\end{aligned} \tag{19}$$

Furthermore, it can be concluded that the steady-state phase difference intervals between the three exciters under the vibration synchronization state are

$$\begin{aligned}
&\vartheta_{20} - \vartheta_{10} + \beta_1 + \beta_2 \in \left[-\frac{\pi}{2}, \frac{\pi}{2}\right]\\
&2\vartheta_{20} - \vartheta_{30} + 2\beta_2 + \beta_3 \in \left[-\frac{\pi}{2}, \frac{\pi}{2}\right]
\end{aligned} \tag{20}$$

TABLE 2. Main parameters of the vibrating system.

Parameter	Symbol	Value	Unit
Moment of inertia of the vibrating system	J	56.5	kg*m^2
Total mass of the vibrating system	M	236.6	kg
Stiffness coefficient in x direction	k_x	100	kN/m
Stiffness coefficient in y direction	k_y	160	kN/m
Damping coefficient in x direction	c_x	0.305	kN*s/m
Damping coefficient in y direction	c_y	0.282	N/mm
Distance from a connecting point between spring and frame to mass-center o	l_s	0.525	m
Distance from the axis of the exciter $i(i=1,2,3)$ to the mass center o	l_i	0.68, 0.33,0.72	m
Angle between the connection of the axis of the Exciter $i(i=1,2,3)$ to the mass center o and the horizontal direction	δ_i	10.2, 21.3, 170.4	degree

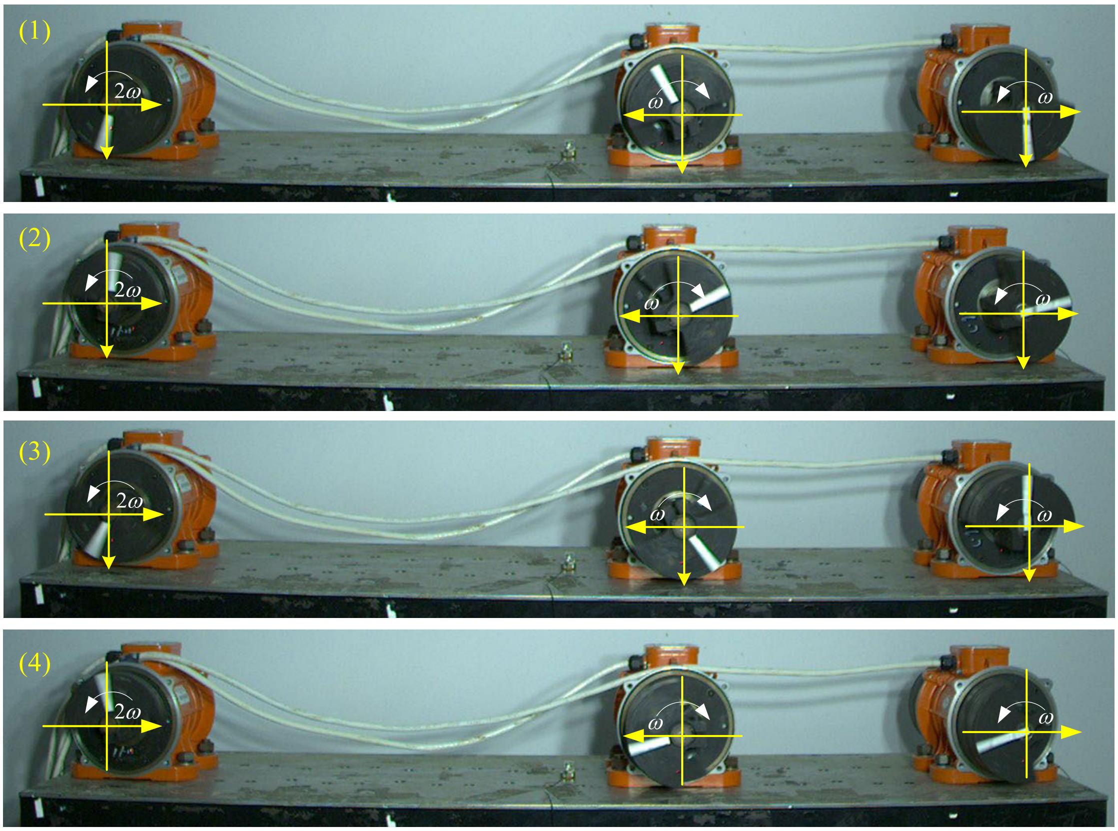

FIGURE 5. Instantaneous phase of the exciters at $n_1 = +600$ rpm, $n_2 = -600$ rpm, $n_3 = +1200$ rpm.

(20) not only gives the stable phase difference relations of the three exciters but also shows that the existence of angle β_i $(i = 1, 2, 3)$ in the equation indicates that the location and the rotational direction of the exciters have obvious influence on the phase differences of the exciters in multi-frequency vibration synchronization system.

In summary, the synchronization criterion and the stability of the synchronization state of the two times frequency vibrating system driven by three exciters are proved. As for the other multi-frequency system, the corresponding synchronization criterion and its stability criterion can be obtained by the similar methods above.

III. EXPERIMENTAL ANALYSIS

From the previous analysis, it can be seen that the key techniques for researching the vibration synchronization system are finding out whether the synchronization state can be achieved, the relations of the phase difference among the

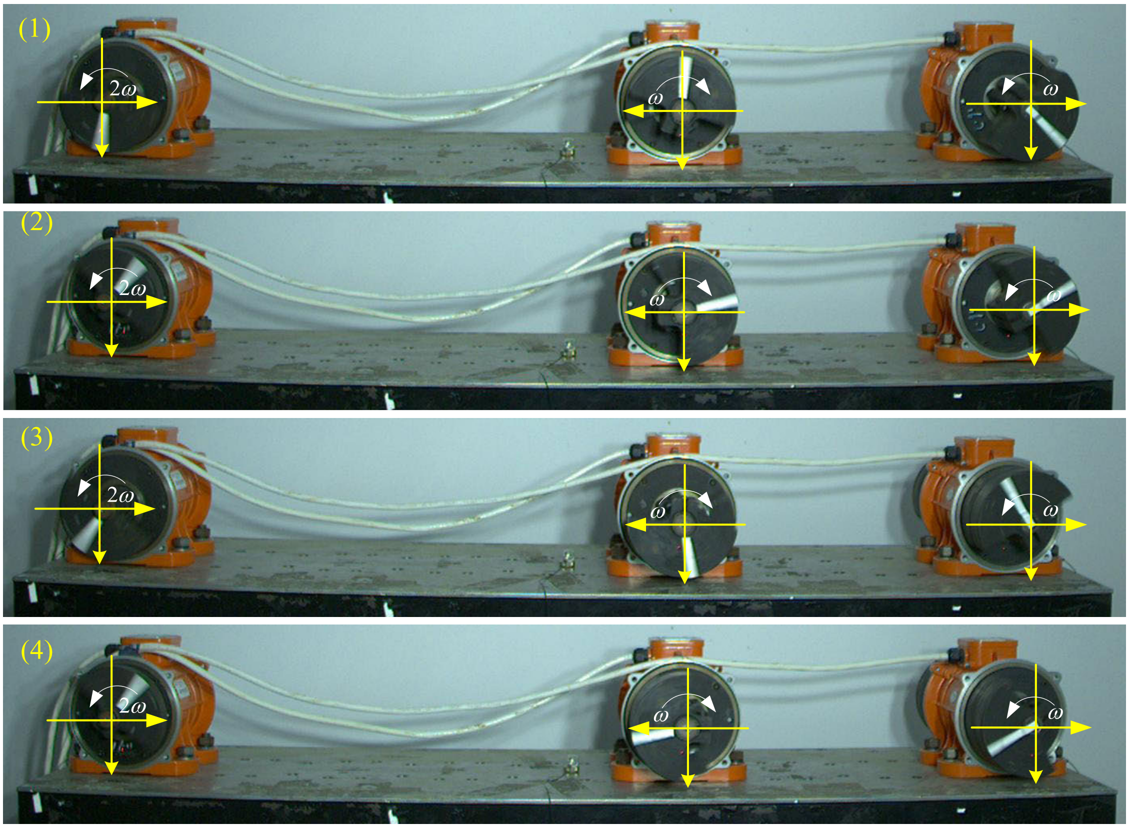

FIGURE 6. Instantaneous phase of the exciters at $n_1 = +700$ rpm, $n_2 = 700$ rpm, $n_3 = +1400$ rpm.

exciters under the steady-state, and the stability of the synchronization state. To prove them from the experimental point of view, an experimental platform is constructed according to FIGURE 3, as shown in FIGURE 4. It should be noted that the three exciters arranged on the same plane have different locating parameters l_i and δ_i. Thus, the experimental platform in FIGURE 4 is consistent with the dynamic model plotted in FIGURE 3. It mainly includes the multi-frequency vibrating system, signal acquisition system, High-speed camera system and some sensors. To obtain the elliptical trajectory required by the screening machinery, the Exciter 1 and Exciter 2 are set as the exciters of low-frequency with large amplitude at the feeding end; the Exciter 3 is set as the exciter at the discharging end powered by two times frequency power supply.

The main parameters of the exciters and the vibrating system are listed in Table 1 and Table 2, respectively. It is worthy to note that the mass and radius of the three exciters are not the same in Table 2. To obtain a more complex trajectory, the $m_i r_i$ of Exciter 1 and Exciter 2 are larger than that of Exciter 3.

First and foremost, What we care about is whether the synchronization state can be achieved. It is a relatively simple way to use the high-speed camera to capture the photos in the operation process of the system. Two sets of experiments with reference speed $n = 600$ rpm and $n = 700$ rpm will be used. To further make the instantaneous phase relationship between the exciters at vibration synchronization state more intuitive and visual, the motion of the exciters is referred to a rectangular coordinate system and uses the mass center of blocks of Exciter 1 passing the coordinate axis in a single circle as a reference.

Basler acA1440-220uc camera(frame rate: 227fps) is used to capture the images, more than 2000 images (6.53GB) are captured in each group experiment. It is not reality to list all the images in a manuscript. Thus, we take the strategy of selecting the images at the same time interval. The real-time photos of the eccentric block of the exciters at steady-state when $n = 600$rpm and $n = 700$rpm are shown in FIGURE 5 and FIGURE 6.

As shown in FIGURE 5 and FIGURE 6, the real-time photos show that the incremental angle of Exciter 3 is always close to 180 degrees when the Exciter 1 and Exciter 2 rotate close to 90 degrees. It illustrates that the phase difference of the two times frequency vibration system on the micro-scale is nearly constant. Thus, the stability of the multi-frequency vibration synchronization state can be guaranteed.

Subsequently, the stable phase difference among the exciters should be investigated. It is worthy to note that the coefficient δ_i $(i = 1, 2, 3)$ listed in Table 2, $\beta_1 + \beta_2$ and $2\beta_2 + \beta_3$ should belong to the phase interval $(-0.5\pi, -1.5\pi)$. Therefore, according to (20), the steady-state phase difference of $\varphi_2 - \varphi_1$ between the Exciter 1 and Exciter 2 should

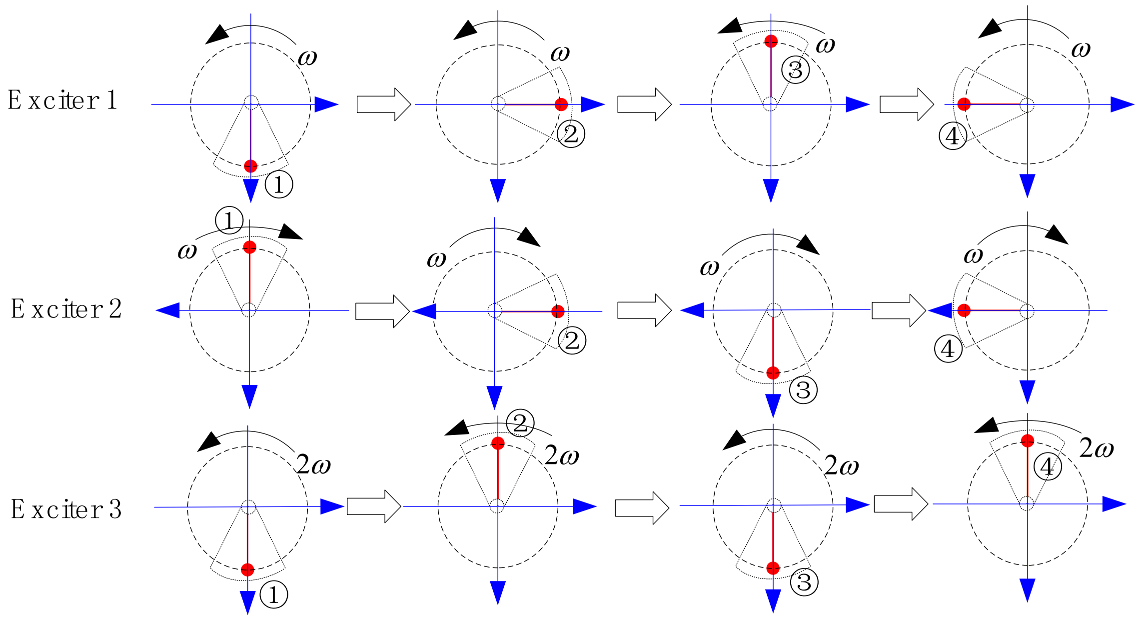

FIGURE 7. Relations of the phase difference of the three exciters in a single cycle period under the condition of anti-phase synchronization.

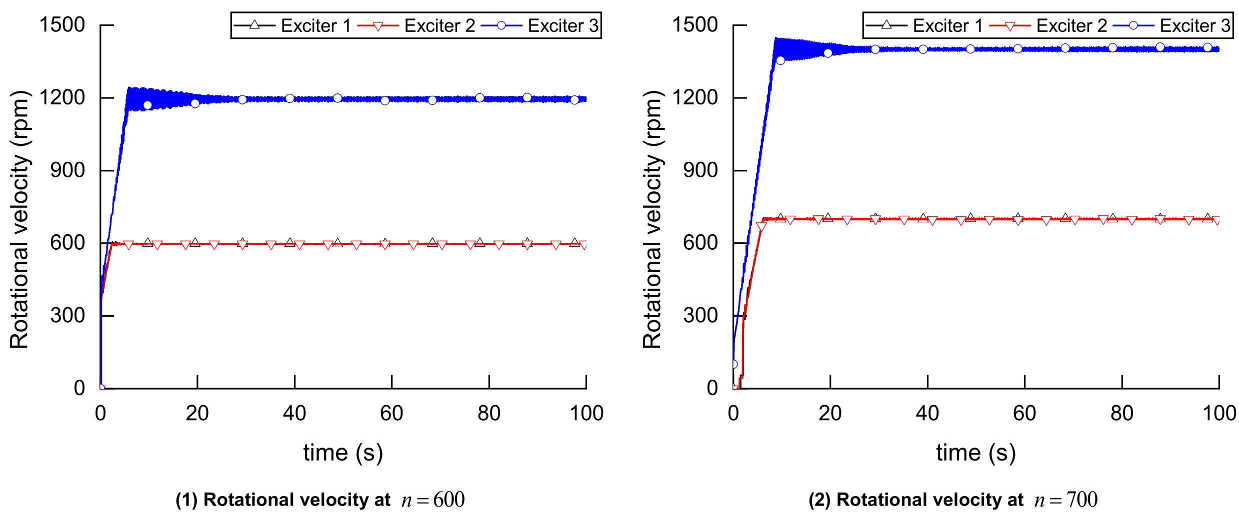

FIGURE 8. Rotational velocity of the exciters over time.

be laid in the interval $(0.5\pi,\ 1.5\pi)$ as the same as phase difference of $2\varphi_2 - \varphi_3$ between the Exciter 2 and Exciter 3. That is, the synchronization state of the system should belong to anti-phase synchronization. More specifically, there is about 180 degrees phase difference, which corresponds to the opposite relational direction and the same relational velocity between Exciter 1 and Exciter 2. Meanwhile, the eccentric block of the exciters turns the same angles at the same time interval. For the Exciter 1 and Exciter 3, which have the same rotational direction, the rotational angles should have obvious two times relations after starting from the same starting point.

According to the analyzed above, the ideal instantaneous phase relations among the exciters at two times frequency vibration synchronization state can be listed as FIGURE 7 when the phase differences between the Exciter 1 and Exciter 2 approaches to π.

Comparing the three figures above, FIGURE 5 and FIGURE 6 denote similar motion phenomena as plotted in FIGURE 7. Due to the coefficient δ_i $(i = 1, 2, 3)$ is not exactly close to zero degree or 180 degrees, the phase difference among the three exciters is close to zero degree or 180 degrees, respectively.

All in all, It can be seen from the above analysis, these phenomena obtained by the high-speed camera can verify the theoretical analysis from a general view. To further master the precise value of the phase difference of the system at steady-state, the rotational velocity of the three exciters over time is given in FIGURE 8 at $n = 600$rpm and $n = 700$rpm.

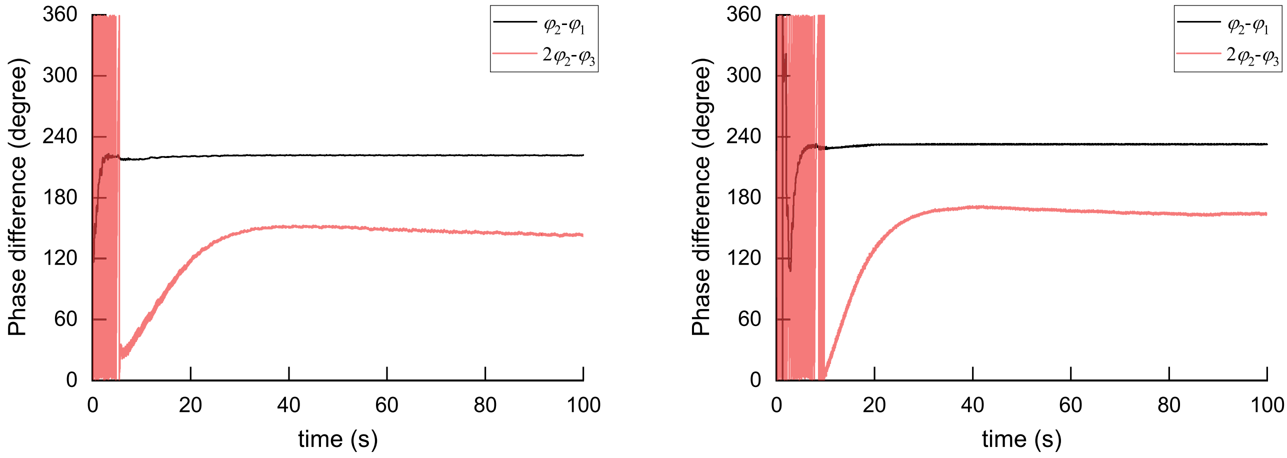

(1) Rotational velocity at $n = 600$ (2) Phase difference at $n = 700$

FIGURE 9. **Phase difference between the three exciters.**

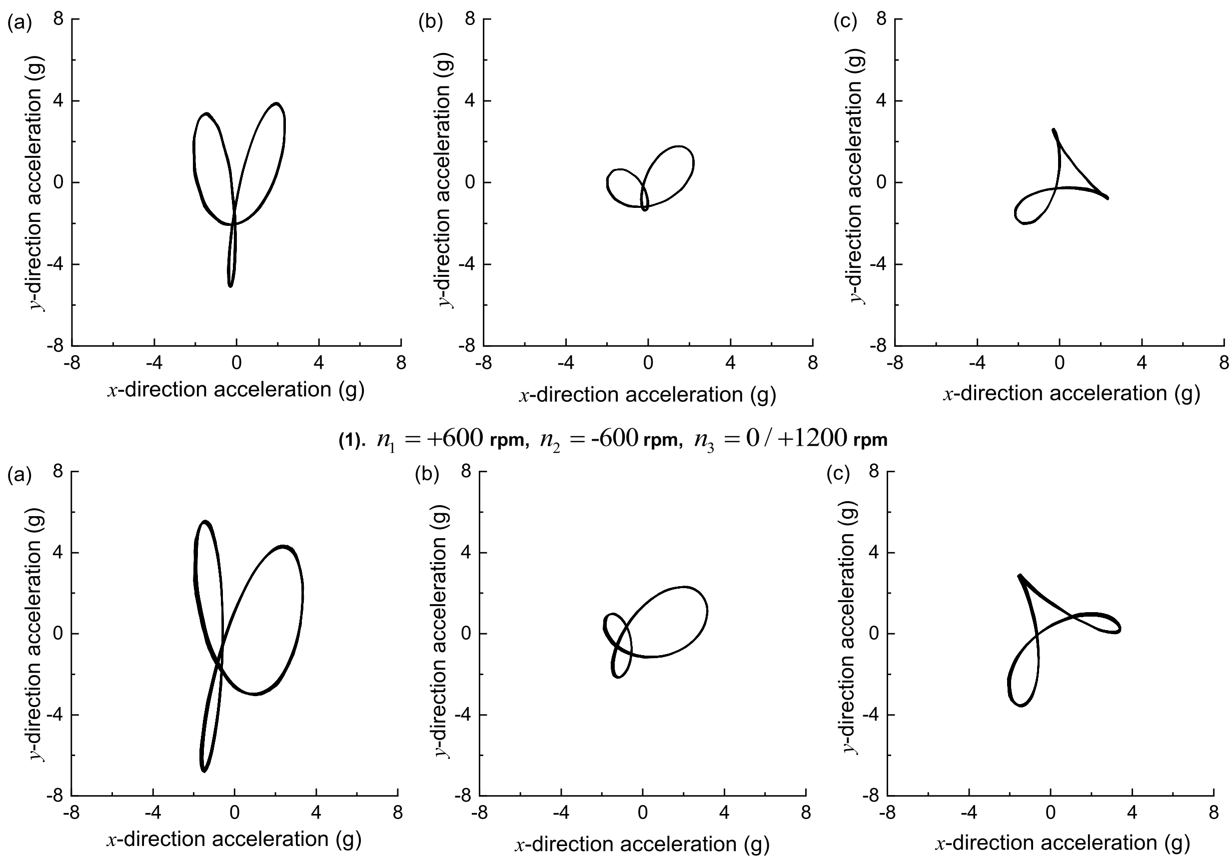

(1). $n_1 = +600$ rpm, $n_2 = -600$ rpm, $n_3 = 0/+1200$ rpm

(2). $n_1 = +700$ rpm, $n_2 = -700$ rpm, $n_3 = 0/+1400$ rpm

FIGURE 10. **Trajectory of exciting force at different position of the vibrating system.**

FIGURE 9 gives out the variation curve of phase differences among the three exciters over time from the system startup to enter the vibration synchronization state.

For the two times frequency vibration system, it can achieve a steady-state of vibration synchronization after about thirty seconds, as shown in FIGURES 8-9. They also show that the phase difference and rotational velocity of the same frequency power supply exciters can be stabilized more quickly than that of the two times frequency exciters. Besides, FIGURE 9 also shows that the steady-state phase difference

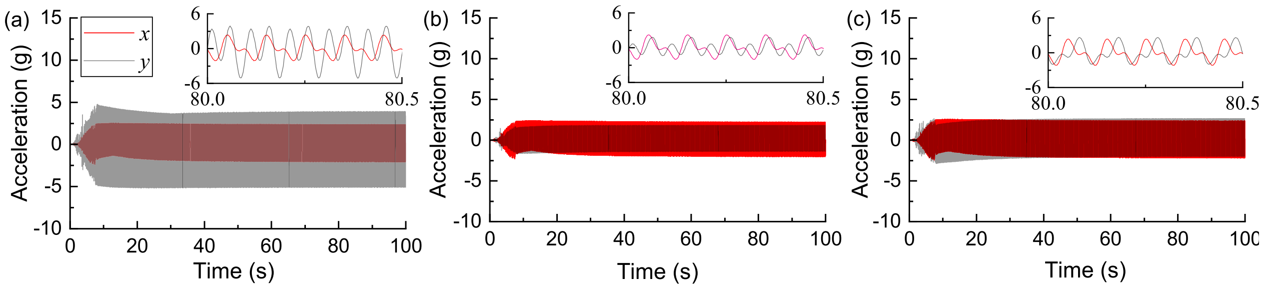

FIGURE 11. Time-domain response of the system at $n_1 = +600$ rpm, $n_2 = -600$ rpm, $n_3 = +1200$ rpm.

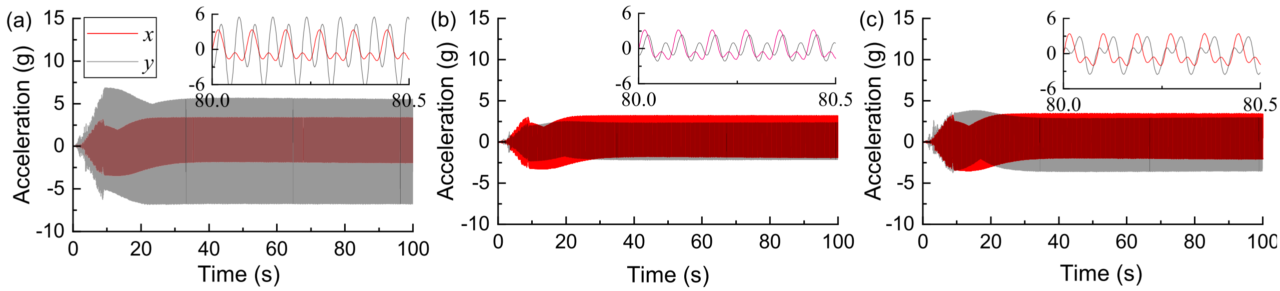

FIGURE 12. Time-domain response of the system at $n_1 = +700$ rpm, $n_2 = 700$ rpm, $n_3 = +1400$ rpm.

of the three exciters is not exactly equal to 180 degrees because of the existence of the angle β_i. These phenomena are consistent with what we theoretically analyze above.

The realization of two times vibration synchronization means that it can be further considered in engineering applications. Corresponding to the standpoint of this paper, we can further research the nonlinear trajectory of the screen. When the selected system achieves the time-frequency vibration synchronization state, the exciting force at different positions when $n = 600$ rpm and $n = 700$ rpm are given in FIGURE 10 with a time interval of 25 seconds. In FIGURES 11-12, the time-domain responses of the exciting force of the system are given, respectively. The positive sign denotes the counterclockwise rotational direction of the Exciter 1 and Exciter 3, and the negative sign denotes the clockwise rotational direction of the Exciter 2.

From FIGURE 10, it can be seen that the whole trajectory of the vibrating system is more complex than a single trajectory of elliptical or linear at two times frequency vibration synchronization states. Compared to our previous experiments in reference [26], the acceleration responses in FIGURE 10 show vertical symmetry, and the middle position gets a relatively small value. These kinds of trajectories driving by more than two exciters with an asymmetric structure in the vibrating system have remarkable engineering efficiency of improving the installed capacity of vibrating machines. Besides, the elliptic trajectory of displacement response is more useful than the circle trajectory for vibration screening system and grinding system, etc.

It is also noteworthy that the exciting force of the leftmost end of the body is larger and complex than other positions under the condition of multi-frequency synchronization. It means that the probability of contact among the granular block materials near the discharge end and the screen surface is further increased. At the same time, the trajectory of granular material is more complex, which can further increase the penetration sieve rate. Besides, compared with the single trajectory, the complex trajectory can further prevent the viscous granular material from clogging the screen hole. These innovation points show that it is feasible and effective to apply the theory of multi-frequency vibration synchronization to the design of the screening machinery to improve screening efficiency. The advantage of the design of multi-frequency machinery by the theory of vibration synchronization is that it makes the structure more simple and easy to control than the current design of the multi-frequency system by the use of more layers frame or vibrating bodies.

IV. CONCLUSION

Asymmetric structure vibrating machines have been widely used in industries. Based on the research background of the elliptical vibrating screen, the concept of multi-frequency screening is put forward, the mechanical model of the multi-frequency vibration synchronization system driven by three motors is established. The asymptotic methods in nonlinear vibration theory proposed by N. N. Bogolyubov and Y. A. Mitropol'skii are introduced for theoretical research. According to the above theoretical derivation and experimental research. Some useful conclusions can be given as follows.

Firstly, the working principle of the elliptical vibrating screening system driven by two exciters is analyzed, a new design to improve the screening efficiency is pointed out, that is, to add a high frequency exciter with small amplitude at the discharge end so as to reduce the clogging of the screen hole and separate viscous block granular particles quickly and effectively. Then the mechanical model of the multi-frequency screening system is present.

Subsequently, by establishing the equation of kinetics, potential energy and energy dissipate function of the system, the differential motion equation of the system is obtained. The motor motion equation with small parameters is obtained by solving the motion equation of the system and setting up the small parameter. By introducing dimensionless time τ, the second-order differential equation of motor motion is transformed into the standard form of the first-order differential equation.

Then, the phase relations of the eccentric block of the exciter is obtained by solving the second-order approximate solution of the motor motion equation and applying the averaging principle. Then the steady-state phase relations of the two times frequency vibration synchronization are obtained. By introducing small perturbation terms μ_i and η_i, linearizing the equation by Taylor expansion, and the theory of nonlinear system, the stability of the vibration synchronization state. Also, the functional relation that the location and the rotational direction of the exciters influence on the phase differences of the exciters are given out.

Finally, according to the mechanical model studied, the corresponding experimental platform is established. Two times frequency vibrations synchronization at $n = 600$ and $n = 700$ are taken as an example to verify the theoretical research. The experiment proves that multi-frequency vibration synchronization with three exciters can be achieved.

From the theoretical analysis and experiment, it is a remarkable fact that the trajectories of the system in different locations mainly rely on the synchronization state, the value $m_i r_i$ of exciters, the multiple synchronous relationships of power supply and the reasonable installation position of exciters. Alternative ideal solutions for the multi-frequency system can be obtained by adjusting the above items. For example, a closer ellipse trajectory for the system in FIGURE 3 needs to adjust the value of $m_3 r_3$ smaller; an in-phase synchronization state usually is favorable to the symmetrical layout of the exciters with opposite relational direction.

REFERENCES

[1] I. I. Blekhman, "Self-synchronization of vibrators in some types of vibration machines," *Inzhenerny*, vol. 16, pp. 49–72, 1953.

[2] I. I. Blekhman, *Synchronization in Nature and Technology*, 1st ed. New York, NY, USA: ASME Press, 1988.

[3] I. I. Blekhman, A. L. Fradkov, H. Nijmeijer, and A. Y. Pogromsky, "On self-synchronization and controlled synchronization," *Syst. Control Lett.*, vol. 31, pp. 299–305, Oct. 1997.

[4] I. I. Blekhman and V. S. Sorokin, "On the separation of fast and slow motions in mechanical systems with high-frequency modulation of the dissipation coefficient," *J. Sound Vib.*, vol. 329, no. 23, pp. 4936–4949, Nov. 2010.

[5] X. Zhang, B. Wen, and C. Zhao, "Theoretical study on synchronization of two exciters in a nonlinear vibrating system with multiple resonant types," *Nonlinear Dyn.*, vol. 85, no. 1, pp. 141–154, Jul. 2016.

[6] X. Zhang, J. Xu, C. Zhao, and B. Wen, "Synchronization of dual homodromy rotors with eccentric masses in a nonlinear vibrating system," *Trans. Can. Soc. Mech. Eng.*, vol. 40, no. 3, pp. 303–315, Sep. 2016.

[7] L. Li and X. Chen, "Double synchronization states of two exciters with horizontal asymmetric structure in a vibrating system," *J. Vibroeng.*, vol. 19, no. 5, pp. 3883–3894, Aug. 2017.

[8] X. Zhang, C. Li, Z. Wang, and S. Cui, "Synchronous stability of four homodromy vibrators in a vibrating system with double resonant types," *Shock Vib.*, vol. 2018, Dec. 2018, Art. no. 9641231, doi: 10.1155/2018/9641231.

[9] C. Zhao, Q. Zhao, Y. Zhang, and B. Wen, "Synchronization of two non-identical coupled exciters in a non-resonant vibrating system of plane motion," *J. Mech. Sci. Technol.*, vol. 25, no. 1, pp. 49–60, Jan. 2011.

[10] J. A. Acebrón, L. L. Bonilla, and R. Spigler, "Synchronization in populations of globally coupled oscillators with inertial effects," *Phys. Rev. E, Stat. Phys. Plasmas Fluids Relat. Interdiscip. Top.*, vol. 62, no. 3, pp. 3437–3454, Sep. 2000.

[11] A. N. Djanan, B. N. Nbendjo, and P. Woafo, "Self-synchronization of two motors on a rectangular plate and reduction of vibration," *J. Vib. Control*, vol. 21, no. 11, pp. 2114–2123, Aug. 2015.

[12] P. Fang, Y. Hou, and Y. Nan, "Synchronization of two homodromy rotors installed on a double vibro-body in a coupling vibration system," *PLoS ONE*, vol. 10, no. 5, May 2015, Art. no. e0126069.

[13] B. C. Wen, H. ZHang, S. Y. Liu, Q. He, and C. Y. Zhao, *Theory and Techniques of Vibrating Machinery and Their Applications*. Beijing, China: Science Press, 2010.

[14] R. Modrzewski and P. Wodzinski, "Analysis of screening process of crushed basalt performed by a double-frequency screen," *Physicochem. Problems Mineral Process.*, vol. 49, no. 1, pp. 81–89, 2013.

[15] R. Modrzewski and P. Wodziński, "The results of process investigations of a double-frequency screen," *Physicochem. Problems Mineral Process.*, vol. 44, pp. 169–178, 2010. [Online]. Available: http://apps.webofknowledge.com/full_record.do?product=UA&search_mode=GeneralSearch&qid=1&SID=6Ebg1V2llgKBgzC92aC&page=1&doc=3 and https://www.infona.pl/resource/bwmeta1.element.baztech-article-BAT6-0013-0016

[16] E. Kremer, "Slow motions in systems with fast modulated excitation," *J. Sound Vib.*, vol. 383, pp. 295–308, Nov. 2016.

[17] X. Zhang, Z. Wang, Y. Zhu, J. Xu, and B.-C. Wen, "Synchronization and stability of two pairs of reversed rotating exciters mounted on two different rigid frames," *IEEE Access*, vol. 7, pp. 115348–115367, 2019.

[18] X. Zhang, B. Wen, and C. Zhao, "Vibratory synchronization transmission of a cylindrical roller in a vibrating mechanical system excited by two exciters," *Mech. Syst. Signal Process.*, vol. 96, pp. 88–103, Nov. 2017.

[19] N. Zhang, "Effect of phase difference on dynamic characteristics for a synchronous vibrating system with double eccentric rotors," *J. Low Freq. Noise, Vib. Act. Control*, vol. 38, no. 2, pp. 473–486, Jan. 2019.

[20] J. Inoue and Y. Araki, "On the self-synchronization of mechanical vibrators : Part6, multiple synchronization," *Trans. Jpn. Soc. Mech. Eng.*, vol. 42, no. 353, pp. 111–117, 1976.

[21] L. Jia, X. Kong, J. Zhang, Y. Liu, and B. Wen, "Multiple-frequency controlled synchronization of two homodromy eccentric rotors in a vibratory system," *Shock Vib.*, vol. 2018, Jun. 2018, Art. no. 4941357, doi: 10.1155/2018/4941357.

[22] W. Qin, X. Jiao, and T. Sun, "Synchronization and anti-synchronization of chaos for a multi-degree-of-freedom dynamical system by control of velocity," *J. Vib. Control*, vol. 20, no. 1, pp. 146–152, Jan. 2014.

[23] Z. Huang, Y. Li, G. Song, X. Zhang, and Z. Zhang, "Speed and phase adjacent cross-coupling synchronous control of multi-exciters in vibration system considering material influence," *IEEE Access*, vol. 7, pp. 63204–63216, 2019.

[24] *Fives Intralogistics Corp*. Accessed: Nov. 7, 2019. [Online]. Available: https://www.fivesgroup.com

[25] M. Zou, P. Fang, H. Peng, D. Hou, M. Du, and Y. Hou, "Study on synchronization characteristics for self-synchronous vibration system with dual-frequency and dual-motor excitation," *J. Mech. Sci. Technol.*, vol. 33, no. 3, pp. 1065–1078, Mar. 2019.

[26] L. Li and X. Chen, "Times-frequency synchronization of two exciters with the opposite rotating directions in a vibration system," *J. Sound Vib.*, vol. 443, pp. 591–604, Mar. 2019.

[27] N. N. Bogolyubov and Y. A. Mitropolskii, *Asymptotic Methods in Nonlinear Vibration Theory*. Moscow, Russia: Nauka, 1974.

[28] B. P. Lathi, *Linear Systems and Signals*, 3rd ed. London, U.K.: Oxford Univ. Press, 2005.

[29] H. K. Khalil, *Nonlinear Systems*, 3rd ed. Upper Saddle River, NJ, USA: Prentice-Hall, 2002.

LINGXUAN LI was born in Nanchong, Sichuan, China, in 1984. He received the B.S. degree in mechanism design, manufacturing and automatization from the Southwest University of Science and Technology, China, in 2007, the M.S. degree in vehicle engineering, in 2009, and the Ph.D. degree in mechanical design and theory from the Northeastern University, Shenyang, China, in 2012. He is currently with the School of Control Engineering, Northeastern University at Qinhuangdao, Qinhuangdao, China. He has authored over ten articles in international journals and applied for more than ten Chinese patents. His research interests include synchronization theory, vibration utilization and control engineering, and nonlinear vibrations in engineering.

XIAOZHE CHEN received the M.S. and Ph.D. degrees from the School of Mechanical Engineering and Automation, Northeastern University, Shenyang, China. He is currently with the School of Control Engineering, Northeastern University at Qinhuangdao, Qinhuangdao, China. His research interests include dynamics of multibody systems, and vibration in mechanics and dynamics of synchronization systems.